P11A.4 AN OBSERVATIONAL STUDY ON THE KINEMATIC CHARACTERISTICS OF RAINBAND OVER CHANGMA FRONTAL ZONE USING DUAL DOPPLER RADAR ANALYSIS

Kyung-Yeub Nam[1*], Kyung-Eak Kim[1], Ji-Hun Park[1], Dong-In Lee[2]
[1]Kyungpook National University, Daegu, South Korea
[2]Pukyong National University, Pusan, South Korea

1. INTRODUCTION

Heavy rainfalls during the summer monsoon are one of the most significant factors in natural disasters and important research topics for meteorologists. It is well known that they frequently occur along the Meiyu (in China), Baiu (in Japan), and Changma (in Korea) frontal zone with a regional difference in locations, timing and duration in the East Asia.

Many studies on the East Asian monsoon system have done in last two decades and can be divided into two categories, based on the scales of observations. One is the sub-synoptic and meso-β scale aspects based on the synoptic observation including the upper air and surface, satellite images, and reanalysis data. Another is the meso-β or meso-γ scale aspects based on the filed experiment data from Doppler radar network, special upper air and wind profiler observations.

Concerning the sub-synoptic scale aspect, it is characterized by the low- and upper-level jet stream, strong moisture gradient, nearly moist neutral stratification and development of sub-synoptic scale frontal depressions with multi-scale features. Moreover, the formation process of the East Asian frontal system was pointed out by the influence of the moisture transport along the western rim of the North Pacific subtropical anticyclone, the convergence/confluence of the monsoon westerly with the Pacific easterly trade wind around the South China Sea, and the middle latitude circulation systems (e.g., Park et al. 1986; Ninomiya and Akiyama 1992; Ding and Johnny 2005).

Regarding the meso-scale aspect, several field experiments have been carried out in the East Asia in order to observe the mesoscale structure of Meiyu/Baiu/Changma frontal precipitation system. In Japan, intensive field experiments using Doppler radars were carried out in Okinawa in 1987, on Kyushu Island in 1988, and on Kyushu Island and over the East China Sea, between 1998 and 2002. The meso-β or meso-γ scale structures of squall lines were analyzed in the experiments (e.g., Ishihara et al. 1995; Yoshizaki 2000). In China, the South China Sea Monsoon Experiment (SCSMEX) was carried out between 1996 and 2001 (e.g., Lau et al. 2001; Ding et al. 2004). The GAME/HUBEX (GEWEX Asian Monsoon Experiment/HUaihe River Basin Experiment, GEWEX: Global Energy and Water Cycle Experiment) using triple Doppler radar analysis was carried out in the Huaihe River Basin in 1998 and 1999 (e.g., Shusse et al. 2005), and in the downstream region of the Yangtze River in 2001 and 2002. The purpose of this experiment was to understand mesoscale features of Meiyu/Baiu frontal convective systems formed in this region (e.g., Yamada et al. 2003; Moteki et al. 2004). In Taiwan, TAMEX (Taiwan Area Mesoscale Experiments) was carried out around Taiwan in 1987 (e.g., Lin et al. 1991; Teng et al. 2000). In Korea, The KORMEX (Korean Mesoscale Experiment) was carried out in the middle of the Korean Peninsula in 1997 and 1998 (Oh et al. 1997) and the KEOP (Korean Enhanced Observing Program) was carried out in the southern part of the Korean Peninsula from 2001 to present (Choi et al. 2006).

Many studies have done on the conditions of synoptic scale disturbances produced heavy rainfalls. However, there are few studies on the mesoscale disturbances occurring over the Korean Peninsula, based on the radar observations. The purpose of the present study is to investigate the kinematical variation of a meso-β scale disturbance observed by dual Doppler radars located in the southern part of the Korean Peninsula.

2. DATA AND METHODS

The summer monsoon of the Korean Peninsula starts in the southern region ocean off from Jeju Island around the middle of June. Therefore, the Island is a good location to study an early phase of the meso-scale disturbances occurred by the Changma frontal precipitation system. The data was obtained during the periods of KEOP, 21 June to 5 July 2006, which was focused on analysis of the change of the disturbance configuration, variation of wind field and rainfall intensity distribution including topographic effect on the disturbance. During the periods of KEOP, five rainfall events were occurred. In this study, the rainfall event of 1 July was investigated. The daily accumulated rainfall amount exceeded more than 110 mm at two stations and 80 mm at 6 other stations. The mesoscale and intensive observational network over the southern part of the Korean Peninsula were shown in Fig. 1. In Fig. 1a, Doppler weather radar (◆), surface (●), and upper-air (■) observation network were shown. The coverage of R1 (Gosan) and R2 (Sungsanpo) radars was drawn by solid line. The available wind retrieval regions using the dual Doppler radar analysis were shaded with green. The rectangular area in Fig. 1a is enlarged in Fig. 1b. The Automatic Weather Stations (AWS, ▲) were shown in Fig. 1b.

* *Corresponding author address*: Kyung-Yeub Nam, Kyungpook National Univ., Dept. of Astronomy and Atmospheric Sciences, Daegu, South Korea 702-701; e-mail: kynam@metri.re.kr

The radar data obtained at Gosan and Sungsanpo were interpolated to Cartesian grids using the Sorted Position Radar Interpolation (SPRINT) software (NCAR 1999) and the Custom Editing and Display of Reduced Information in Cartesian Space (CEDRIC) software package (Miller and Fredrick 1998). The horizontal and vertical grid intervals were 1 and 0.5 km, respectively.

Particle fall speeds were estimated from the reflectivity (Biggerstaff and Houze, 1991) and vertical velocity was computed from the an-elastic equations of continuity (O'Brien, 1970). Because of Mt. Halla located on the center of Jeju Island, Gosan and Sungsanpo radars have the beam blocking area from 55˚ to 100˚, from 260˚ to 320˚ of azimuth, respectively. To cover the area, the reflectivity of two radars was merged with the maximum value in the overlapped area.

Synoptic conditions have been made using the global reanalysis data from the National Centers for Environmental Prediction–National Center for Atmospheric Research (NCEP–NCAR). These data are provided on 2.5˚ × 2.5˚ grids at 17 vertical levels from 1000 hPa to 10 hPa every 6 hours.

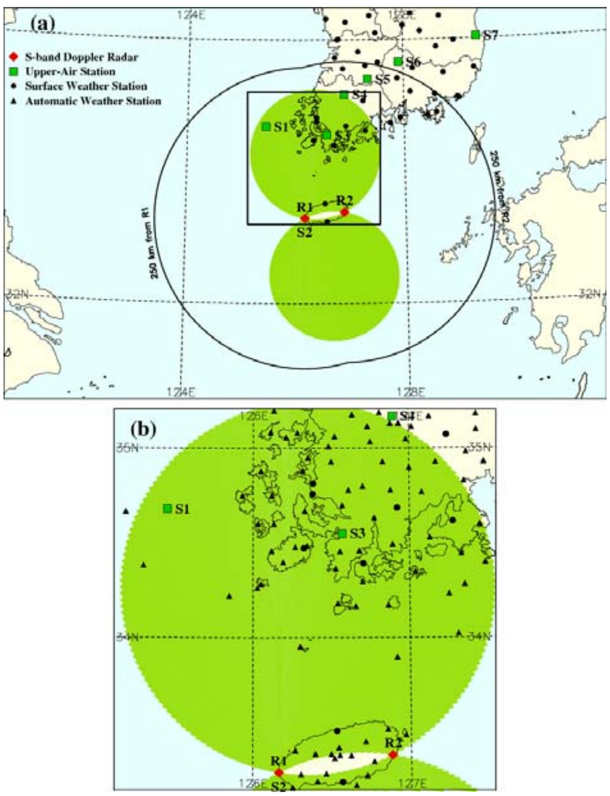

Fig. 1. (a) Mesoscale and (b) intensive observational network of the southern part of the Korean Peninsula.

3. RESULTS

The analyzed system was originated near Jiangsu, northern downstream region of Yangtze River of China, at 2300 LST 30 June 2006 and propagated to the middle of Japan. It arrived the southern part of the Korean Peninsula at 0800 LST 1 July 2006 and moved eastward along Changma front oriented from the southwest to the northeast (Fig. 2). In Fig. 2, the inversely highlighted regions denote the regions of the analyzed convective system, which were blow -43℃ brightness temperature. At 0500 LST, it has become organized into a strong convection over the Yellow Sea and another cluster of convective cells have developed over China and the Korean Peninsula. The strong convective system has landed to the southern part of the peninsula at 0800 LST.

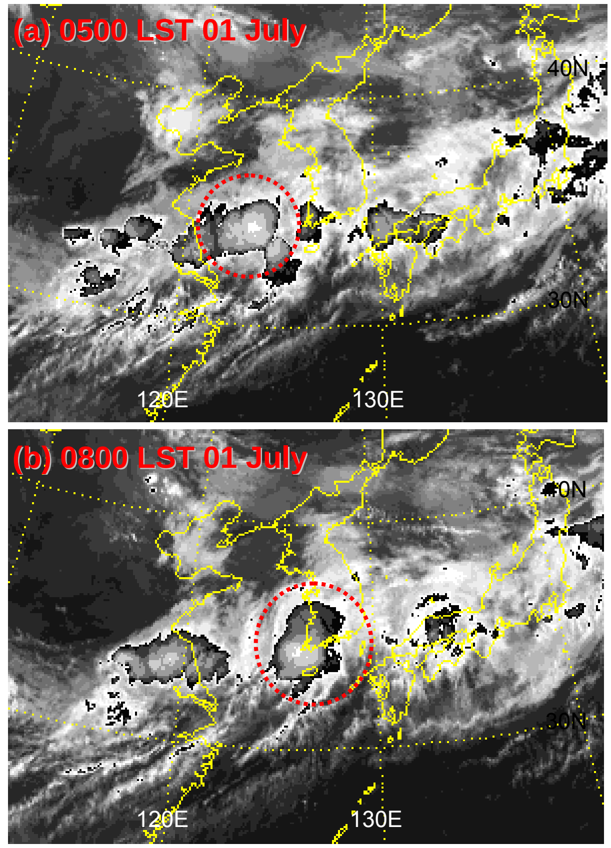

Fig. 2. The enhanced infrared images of MTSAT-1R satellite at 0500, 0800, and 1300 LST 01 July 2006.

The synoptic condition of mature stage is shown in Fig. 3. The solid lines denote the sea level pressure (hPa, contoured every 2 hPa) in Fig. 2a, the equivalent potential temperature (K, contoured every 3 K and greater than 333 K) in Fig. 3b, the relative vorticity (10^{-5} s^{-1}, contoured every $2\times10^{-5}s^{-1}$), and the geopotentail height (m, contoured very 50 m) in Fig. 3d. Winds are indicated by arrows. The shaded areas represent the precipitable water (kgm^{-2}) of the entire atmospheric column in Fig. 3a and the wind speed greater than 8, 12, 12 and 20 ms^{-1} in Fig. 2b though Fig. 3d, respectively. In Fig. 2b, the box is the area of dual Doppler radar analysis.

The surface weather map shows that an extensive trough was formed between the western Pacific subtropical high (WPSH) and the continental high. The precipicitable water (≥ 4.5 kgm^{-2}) is found along the flank of WPSH. The equivalent potential temperature at 850 hPa shows that the large-scale condition produces a narrow channel of moist-air transport from southern China to the Korean Peninsula. At 850 hPa, an extended belt of strong southwesterly is found along the flank of anti-cyclonic circulation associated with the WPSH (Fig. 3b). Cyclonic circulation associated with the 850 hPa trough is found to the north of the peninsula. Relatively strong gradients of height at 300 hPa are found at the northern part of China (Fig. 3d). The distribution of relative vorticity at 500 hPa shows that the northern part of low level jet (shaded region at 850 hPa) is positive and its southern part is negative.

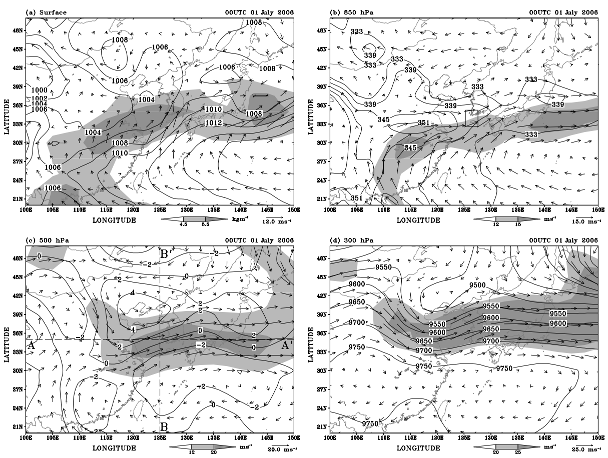

Fig. 3. NCEP-NCAR reanalysis charts for (a) surface, (b) 850 hPa, (c) 500 hPa, and (d) 300 hPa at 00UTC 01 July 2006.

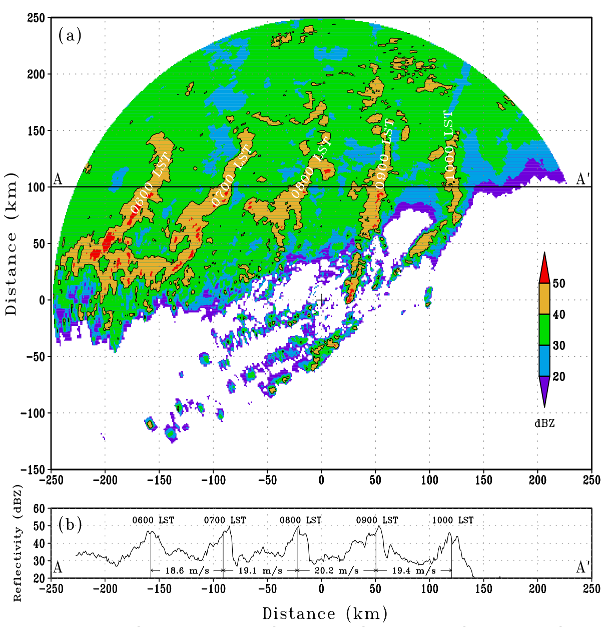

Fig. 4. (a) Composite of 3 km CAPPI reflectivity from 0600 through 1000 LST 1 July 2006 in an hour interval and (b) The reflectivity distribution of cross-section (AA'). The contoured line denotes 40 dBZ.

The horizontal structure and time evolution of the system were observed through the mesoscale radar network. Fig. 4 shows the horizontal distribution of accumulated reflectivity at 3 km level in an hour interval from 0600 to 1000 LST 1 July 2006. Strong convective areas were identified with radar echoes greater than 40 dBZ (Fig. 4a). The horizontal cross-section of AA' in Fig. 4a was used to calculate the motion of system in Fig. 4b and the center of the system was chosen as a mid-point of reflectivity distribution over 40 dBZ every an hour horizontally. It moved toward the east-northeast, which was almost perpendicular to the orientation of the system. These echoes had a blob structure before 0500 LST (not shown). It changed into an arc-shaped convective system originated from the south-southwest to the north-northeast extending more than 150 km after 0600 LST, and lasted to 0700 LST. During its approach to the land, the east-southwestern (rear) edge of the arc-shaped convective system dissipated but the east-northeastern part of it maintained. At 0900 LST, it converted into a line-shaped convective system elongated from north to south due to new convection at the northern part of system. The analyzed system moved toward 80° of azimuthal angle and the motions were 18.6 ms^{-1} at 0700 LST, 19.1 ms^{-1} at 0800LST, 20.2 ms^{-1} at 0900 LST, and 19.4 ms^{-1} at 1000 LST.

The convective system passed the intensive observational region between 0730 and 1000 LST. For the period, the kinematic characteristics of the arc- and line-shaped convective system were investigated. The spatial distribution of the horizontal wind and reflectivity at height of 3 km was shown in Fig. 5. It was oriented in the north-south direction, and consisted of three major regions: one convective rainfall region (≥ 40 dBZ) and two weak stratiform rainfall regions. One weak stratiform rainfall region was ahead of the one convective rainfall region while the other was developed behind the convective region. The southwesterly including the moisture was ahead of the convective region and the westerly, northeasterly and northwesterly including the dry air and wind disturbances was behind it. It has developed the convection.

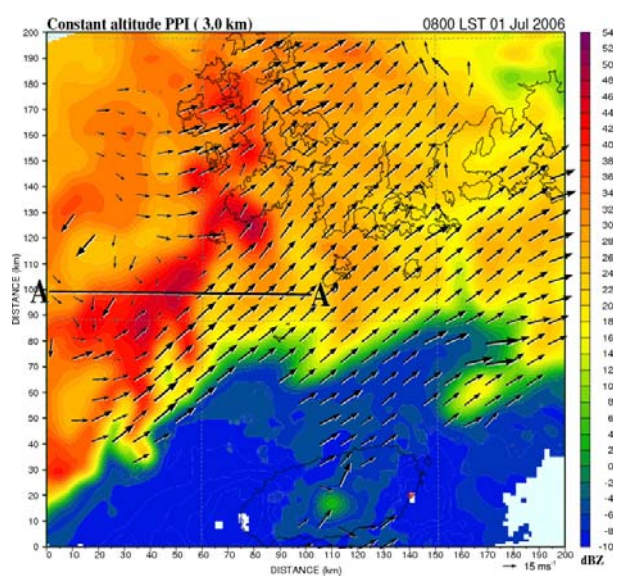

Fig. 5. Horizontal wind and reflectivity at the height of 3 km at 0800 LST 1 July 2006.

Figure 6 shows the vertical cross-section of AA' in Fig. 5. The line-shaped convective system had a weak wind along the upper frontal line (densely contoured line of wind direction) and a disturbance occurred below the altitude of 5 km in the rear of system from 20 to 50 km in Fig. 6b and 6d. During its approach to the Korean Peninsula, the arc-shaped convective system was converted to the line-shaped convective system by the topographic effect and the change of environment around the system. At the distance of 40 – 55 km in Fig. 6, the disturbance at low level greatly enhanced the convection of the system, in which the strong vertical air velocity was over 8 ms^{-1} in Fig. 6a, the strong horizontal wind was over 40 ms^{-1} over the height of 12 km in Fig. 6b, the horizontal convergence (contoured line), 24×10^{-4} s^{-1} and the horizontal vorticity (shaded region), 42×10^{-4} s^{-1} in Fig. 6c. The horizontal convergence enhanced by the southwesterly inflow around the upper frontal line was important to develop the convection by lifting the elevated air that possessed conditional instability. There was a strong vertical wind shear in the system in Fig. 6d. The low level jet located ahead of convective system and the upper level jet located at top of it. Their locations has enhanced the conditional instability and developed the convection (Fig. 6b).

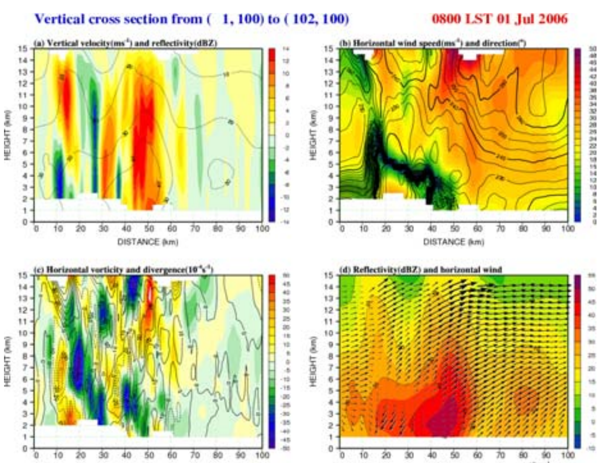

Fig. 6. Vertical cross-section of AA' in Fig. 5 for (a) the vertical velocity and reflectivity, (b) the horizontal wind speed and direction, (c) the horizontal vorticity and divergence, and (d) the reflectivity and horizontal wind.

The northeasterly and northwesterly including the dry air occurred over the rear of the system had been disappeared and the disturbance was modified the westerly at 0900 LST (Fig. 7). At 0900 LST, it has a new convection at the northern part (rear) of system due to the topographic effect of Mt. Halla and then modified into a long line-shaped convective system elongated from north and south. Figure 8 shows the vertical cross-section of AA' of Fig. 7. The horizontally narrow and strong updraft at the upper level of 8 km is found at the distance of 55 km in Fig. 8a. The upper level jet was located at the lower than 0800 LST. The maximum convergence and relative vorticity were weakened to 4×10^{-4} and 18×10^{-4}, respectively. The southwesterly including the moisture was ahead of the convective region and the westerly including the dry air was behind it.

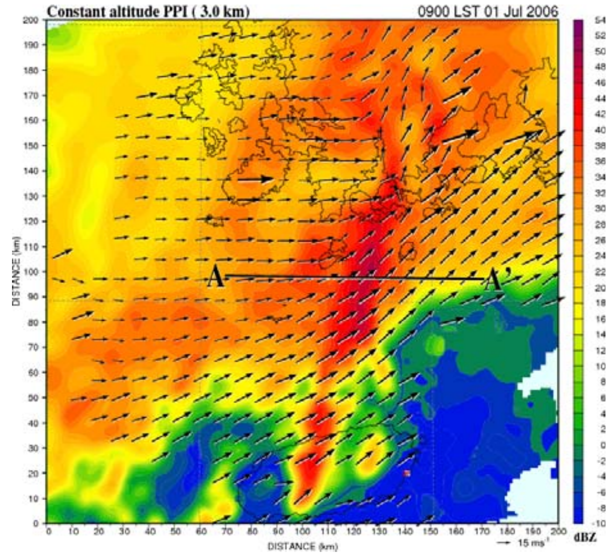

Fig. 7. Same as Fig. 5 except for 0900 LST.

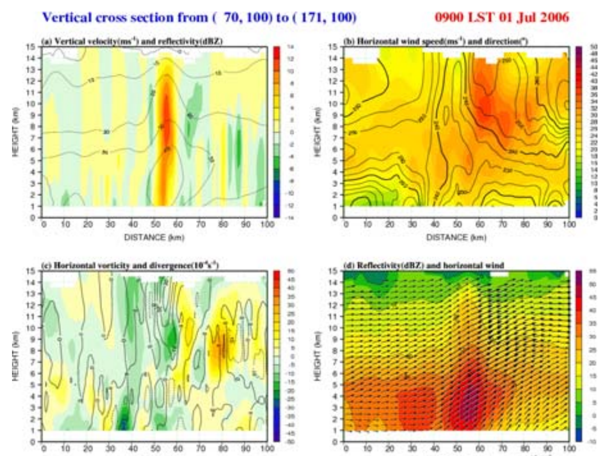

Fig. 8. Same as Fig. 6 except for Fig. 7.

The system began to dissipate after the line-shaped convective system passed the ocean between the Southern boundary of the Korean Peninsula and Jeju Island with Mt. Halla. This is because the topographic effect of Mt. Halla significantly modified both the shape of the convective system and the speed of air flow. During the passing of the system over the ocean, the air flow speed was greatly increased, and then induced a strong divergence, causing the decay of the system.

4. SUMMARY AND CONCLUSIONS

The purpose of the present study is to investigate the kinematical variation of a mesoscale disturbance by Dual Doppler radar observation data, which was obtained during the periods of KEOP (from 21 June to 5 July 2006). The analyzed system was originated near Jiangsu, northern downstream region of Yangtze River of China, at 2300 LST 30 June 2006 and propagated to the middle of Japan. It was oriented in the north-south direction, and consisted of three major regions: one convective rainfall region and two weak stratiform rainfall regions. The maintenance mechanisms of the strong convection were the southwesterly including the moisture, the westerly, northeasterly and northwesterly including the dry air and the disturbance at the rear of the convective system. The horizontal convergence enhanced by the southwesterly inflow around the upper frontal line was important to develop the convection by lifting the elevated air that possessed conditional instability. During approach of the convective system to the Korean Peninsula, the transition of the kinematic characteristics was not studied in detail in this study. The research of it will be performed by the numerical simulation with the high resolution below 1 km horizontally.

5. ACKNOWLEGMENTS

This work was supported by the Korea Foundation for International Cooperation of Science & Technology (KICOS) through a grant provided by the Korean Ministry of Science & Technology (MOST) in 2006 (No. 2006-03874), the "Development of METRI X-band Doppler Weather Radar Operations and Radar Data Analysis Technique" and "Korea Enhanced Observing Program, KEOP" of the National Institute of Meteorological Research (NIMR). NCEP–NCAR reanalysis data were provided by the NOAA–CIRES Climate Diagnostics Center, Boulder, Colorado, from their site online at http://www.cdc.noaa.gov/.

6. REFERENCES

Biggerstaff, M.I. and R.A. Houze, Jr., 1991: Kinematic and precipitation structure of the 10–11 June 1985 squall line. *Mon. Wea. Rev*., **119**, 3034–3065.

Choi, Y.J, S.Y. Lee, K.H. Kim, H.Y. Won, C.G. Park, J.C. Nam, and D.E. Chang, 2006: An overview of the KEOP-2006 IOP (Korea Enhanced Observing Program in 2006) and some highlights, *The 2nd Korea-Japan-China joint conference on meteorology*, Oct. 11-13, 2006, Goyang, Korea.

Ding, Y.H., C.Y. Li and Y.J. Liu, 2004: Overview of the South China Sea monsoon experiment. *Adv. Atmos. Sci.*, **21**, 343-360.

Ding, Y.H and C.L.C. Johnny, 2005: The East Asian summer monsoon: an overview, *Metoerol. Atmos. Phys*., **89**, 117-142.

Houze, R.A. Jr., B.F. Smull, and P. Dodge, 1990: Mesoscale organization of springtime rainstorms in Oklahoma. *Mon. Wea. Rev*., **118**, 613-654.

Ishihara, M., Y. Fujiyoshi, A. Tabata, H. Sakakibara, K. Akaeda and H. Okamura, 1995: Dual Doppler radar analysis of an intense mesoscale rainband generated along the Baiu front in 1988: Its kinematical structure and maintenance process. *J. Meteor. Soc. Japan*, **73**, 139-163.

Lau, K.M., Y.H. Ding, J.T. Wang, R. Johnson, R. Cifelli, J. Gerlach, O. Thjiely, T. Rikebbach, S.C. Tsay and P.H. Lin, 2000: A report of the field operation and early results of the South China Sea monsoon experiment (SCSMEX). *Bull. Amer. Meteor. Soc*., **81**, 1261-1270.

Lin, Y.-J., R.W. Pasken and H.-W. Chang, 1991: The structure of a subtropical prefrontal convective rainband. Part I: Mesoscale kinematic structure determined from dual Doppler measurements. *Mon. Wea. Rev*., **120**, 1816-1836.

Miller, L. J., and S. M. Fredrick, 1998: Custom Editing and Display of Reduced Information in Cartesian space (CEDRIC) manual. National Center for Atmospheric Research, Mesoscale and Microscale Meteorology Division, Boulder, CO, 130 pp.

Moteki, Q., H. Uyeda, T. Maesaka, T. Shinoda, M. Yoshizaki, and T. Kato, 2004: Structure and development of two merged rainbands observed over the East China Sea during X-BIAU-99 PART I: Meso-β-scale structure and development processes. *J. Meteor. Soc. Japan*, **82**, 19-24.

NCAR, 1999: Sorted Position Radar Interpolation (SPRINT) manual. National Center for Atmospheric Research, Mesoscale and Microscale Meteorology Division, Boulder, CO, 76 pp.

Ninomiya, K., and T. Akiyama, 1992: Multi-scale features of Baiu, the summer monsoon over Japan and the East Asia. *J. Meteor. Soc. Japan*, **70**, 467-495.

O'Brien, J.J., 1970: Alternative solution to the classical vertical velocity problem. *J. Appl. Meteor*., **9**, 197-203.

Oh, J.H., W.T. Kwon, and S.B. Ryoo, 1997: Review of the researches on Changma and future observational study (KORMEX). *Adv. Atmos. Sci.*, **14**, 207-222.

Park, S.U., I.H. Yoon, and S.K. Chung, 1986: Heat and moisture sources associated with the Changma front during the summer of 1978. *J. Korean. Meteor. Soc.*, **22**, 1-27.

Shusse, Y.K., K. Tsuboki, B. Geng, H. Minda and T. Takeda, 2005: Structure and evolution of deeply developed convective cells in a long-lived cumulonimbus cloud under a weak vertical wind-shear condition. *J. Meteor. Soc. Japan*, **83**, 351-371.

Teng, J.-H., C.-S. Chen, T.-C.C. Wang and Y.-L. Chen, 2000: Orographic effects on a squall line system over Taiwan. *Mon. Wea. Rev.,* **128**, 1123-1138.

Yamada, H., B. Geng, K.K. Reddy, H. Uyeda, and Y. Fujiyoshi, 2003: Three-dimensional structure of a mesoscale convective system in a Baiu-frontal depression generated in the downstream region of Yangtze River. *J. Meteor. Soc. Japan*, **81**, 1243-1271.